Teagle, D.A.H., Wilson, D.A., Acton, G.A., and Vanko, D.A. (Eds.)
Proceedings of the Ocean Drilling Program, Scientific Results Volume 206

6. Data Report: Trace Element Analyses in Whole-Rock Basement Samples, Site 1256, ODP Leg 206[1]

Kari M. Cooper[2]

ABSTRACT

In this report, I present trace element data for basement samples at Ocean Drilling Program (ODP) Site 1256. The samples analyzed represent a subset of the group ("pool") samples from ODP Leg 206, and these trace element data are part of a more comprehensive data suite for the same samples, with analyses of stable and radiogenic isotopes (e.g., Sr, Li, and O) in progress or recently completed that will be presented elsewhere. The trace element analyses were performed in the GeoAnalytical Lab at Washington State University. The following elements were analyzed: La, Ce, Pr, Nd, Sm, Eu, Gd, Tb, Dy, Ho, Er, Tm, Yb, Lu, Ba, Th, Nb, Y, Hf, Ta, U, Pb, Rb, Cs, Sr, Sc, and Zr. Trace element data indicate that the igneous basement at Site 1256 is geochemically normal mid-ocean-ridge basalt. A massive ponded flow sampled in both Holes 1256C and 1256D is distinguished by higher abundances of rare earth elements (REE) and most of the other trace elements analyzed. One interval of highly altered basalt has significantly higher concentrations of Cs, Rb, and Ba and lower concentrations of Sr, Pb, Zr, Hf, Sc, and most REE than the samples of background alteration or halos. No correlation is obvious between trace element abundance and macroscopic type of alteration within the background alteration or halos.

INTRODUCTION

In this report, I present trace element data for samples of basement core collected during Ocean Drilling Program Leg 206 in Holes 1256C

[1] Cooper, K.M., 2007. Data report: trace element analyses in whole-rock basement samples, Site 1256, ODP Leg 206. *In* Teagle, D.A.H., Wilson, D.S., Acton, G.A., and Vanko, D.A. (Eds.), *Proc. ODP, Sci. Results,* 206: College Station, TX (Ocean Drilling Program), 1–10.
doi:10.2973/odp.proc.sr.206.010.2007
[2] Department of Earth and Space Sciences, University of Washington, 310 Condon Hall Box 351310, Seattle WA 98195, USA. Present address: Department of Geology, University of California, Davis, One Shields Avenue, Davis CA 95616, USA.
kmcooper@geology.ucdavis.edu

Initial receipt: 10 May 2005
Acceptance: 5 September 2006
Web publication: 7 February 2007
Ms 206SR-010

and 1256D. These samples represent a subset of a suite of samples collected and shared by a group of shipboard scientists ("pool" samples), which were powdered at Southampton Oceanography Centre and then split and distributed for analysis. The data array for the suite will consist of a wide range of geochemical analyses on the same powders, ensuring that the different analyses will be directly comparable. The samples are from the igneous basement and represent a range of alteration from background level (slightly altered) to vein-related alteration (halos) to highly altered; the single exception is Sample 206-1256D-4R-1, 13–20 cm, which is a chert from the top of the first rotary core in basement. This sample likely represents a piece of chert from within the sedimentary section immediately above the basement that fell into the hole and was sampled during initial basement coring. All of these samples have also been analyzed for lithium and oxygen isotopic composition, and these data will be discussed along with the trace element data elsewhere (K.M. Cooper et al., unpubl. data). Other geochemical data on the same sample suite are in progress, including strontium isotopes and major elements (R. Coggan and D.A.H. Teagle), chlorine isotopes (M. Bonifacie), nitrogen isotopes (Busigny et al., 2005), and sulfur isotopes and oxygen-isotope analyses of vein minerals (J.C. Alt).

The igneous stratigraphy and shipboard geochemistry of Holes 1256C and 1256D have been described in detail in the Leg 206 *Initial Reports* volume (Shipboard Scientific Party, 2003). Briefly, the section in Hole 1256C consists of 27 m of thin basaltic sheet flows a few tens of centimeters to ~3 m thick, which overlie a 32-m-thick massive ponded flow and an additional ~4 m of thin sheet flows. Coring in Hole 1256D began within a massive flow (Unit 1256D-1), which correlates with the massive flow in Hole 1256C but is more than twice as thick (minimum thickness of 74.2 m). The remainder of the 500 m of section cored in Hole 1256D consists mostly of thin sheet flows (tens of centimeters thick to ~3 m thick) and uncommon massive flows 3.5–16 m thick, with a few intervals of pillow basalt and hyaloclastite recovered. The threshold of 3 m between thin sheet flows and massive flows was a standard agreed to by the Leg 206 shipboard science party and is used in other publications (Shipboard Scientific Party, 2003). Igneous rocks from throughout Holes 1256C and 1256D are slightly to moderately altered, where olivine is replaced and pore spaces filled by saponite and minor pyrite, reflecting low-temperature seawater interaction at low seawater/rock ratios (Shipboard Scientific Party, 2003). One interval of basalt in Core 206-1256D-57R is intensively altered to an assemblage of blue-green phyllosilicate (celadonite?), colorless phyllosilicate, and iron oxyhydroxides and is 80%–90% altered (Shipboard Scientific Party, 2003). Shipboard chemical analyses revealed high Si, Al, Fe, Mg, K, P, Cr, and Ni and low Ca and Mn when normalized to Ti (Shipboard Scientific Party, 2003). Locations for pool samples were chosen in order to cover a range of alteration in the core; in each lithologic unit defined in the igneous basement, we chose at least one sample of the least-altered rock (background sample) for comparison with samples that represented higher degrees of alteration (e.g., halos, patchy alteration, hyaloclastites, or the intensively altered interval). I also analyzed the Leg 206 interlaboratory standard prepared on board the ship (BAS-206).

METHODS

Samples were crushed and powdered at Southampton Oceanography Centre (with the exception of BAS-206, which was ground in tungsten carbide on the *JOIDES Resolution*) and splits were sent to the GeoAnalytical Lab at Washington State University for analysis. Details of the digestion technique and analytical protocols are presented elsewhere (Knaack et al., 1994; see also **http://www.wsu.edu/~geolab/note/icpms.html**). Briefly, the method is as follows.

A rock powder sample (100 mg) is dissolved on a hot plate at 110°C, using a mix of HF, HNO_3, and $HClO_4$ in an open Teflon vial. The sample is evaporated to dryness, followed by an additional evaporation with 2 mL of $HClO_4$ at 165°C to convert insoluble fluorides to soluble perchlorates. The sample is then dissolved in HNO_3 plus trace H_2O_2 and HF, and an internal standard of In, Re, and Ru is added to the sample, which is then is diluted to 60 mL final volume. The samples are run on a Sciex Elan model 250 inductively coupled plasma–mass spectrometer equipped with a Babington nebulizer. In-house rock standards and an acid blank are run with each group of unknown samples. Data reduction is performed offline, and raw intensities are corrected for drift using the In, Re, and Ru internal standards. Calibration curves for each element are constructed from the rock standards and single acid blank. Concentrations for the unknown samples are then computed from this curve.

The following elements were analyzed: La, Ce, Pr, Nd, Sm, Eu, Gd, Tb, Dy, Ho, Er, Tm, Yb, Lu, Ba, Th, Nb, Y, Hf, Ta, U, Pb, Rb, Cs, Sr, Sc, and Zr. Precision (assessed with reference to 50–60 analyses of two different rock standards over a 2-yr period) is 2%–5% for the rare earth elements (REE) and 5%–10% for other trace elements.

RESULTS

Results are presented in Table **T1** and Figures **F1, F2,** and **F3.** Most of the trace elements analyzed (with the exception of Pb and Sc) show a distinct shift from the massive ponded flow in Hole 1256D to deeper flows in the same hole. The two samples of the massive ponded flow in Hole 1256C (Samples 206-1256C-8R-4, 105–112 cm, and 10R-2, 55–64 cm) have trace element chemistry similar to the samples of sheet flows from higher in the igneous section, although the sheet flow beneath the ponded flow in Hole 1256C has lower concentrations of Zr, U, Th, and Hf, lower Zr/Y, and higher Th/U than the samples from the uppermost igneous section (Figs. **F1, F2**). All samples of the igneous basement can be classified as normal mid-ocean-ridge basalt (N-MORB), based on chondrite-normalized La/Sm ratios within the range 0.52–0.73 (Fig. **F2**). REE patterns for all samples of igneous basement are depleted in light REE, and relatively flat in the middle to heavy REE, with most having a negative Eu anomaly (Fig. **F3**). Absolute abundances of REE are higher in the massive ponded flow in Hole 1256D (Unit 1256D-1) than in flows deeper in the section, although the negative Eu anomaly is not notably more pronounced in the ponded flow. Abundances of REE in all basement samples from Hole 1256C are similar to those in the massive ponded flow in Hole 1256D (Fig. **F3B**). The ponded flow in Hole 1256D has higher concentrations of all elements measured (except U, Sr, and Sc) than does the unit immediately below. Ba/La, Zr/Y, Th/U and

T1. Trace element abundances at Site 1256, p. 9.

F1. Trace element abundance vs. depth, p. 6.

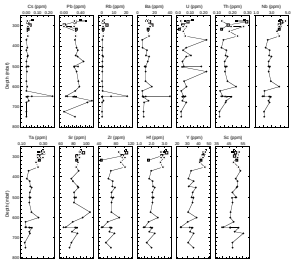

F2. Selected trace element ratios vs. depth, p. 7.

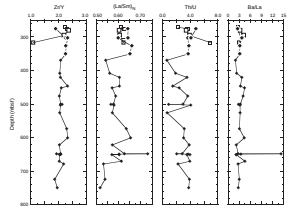

F3. REE abundances normalized to chondritic values, p. 8.

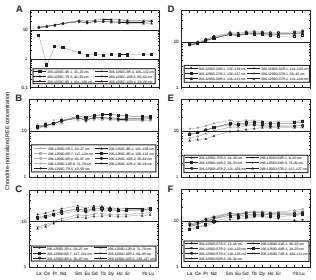

chondrite-normalized La/Sm ratios in samples from Hole 1256C are similar to those in Unit 1256D-1, with the exception of the sheet flow sample below the massive flow in Hole 1256C (Sample 206-1256C-12R-4, 20–26 cm), which has higher Th/U and lower Zr/Y ratios. This sample also has low concentrations of Th, U, Zr, and Hf compared to other samples in Hole 1256C, suggesting that it may contain a refractory phase (e.g., zircon) that was not completely dissolved during analysis. No zircon was found during thin section analysis, but apatite was reported, and a very small percentage of zircon (<<1%) would be sufficient to explain the decrease in Zr, Hf, Th, and U concentrations by the observed amount. There is no apparent difference between the background alteration and halos in terms of trace element abundances or ratios. I analyzed two highly altered samples from a 41-cm-long interval of intensively altered basalt (Samples 206-1256D-57R-2, 117–127 cm, and 57R-3, 13–18 cm). These samples have significantly higher concentrations of the fluid-mobile elements Cs, Rb, and Ba and higher La/Sm, Cs/Pb, and Ba/La ratios than the samples of background alteration or halos (Figs. **F2, F3**). Concentrations of Sr, Pb, Zr, Hf, Sc, and most REE are lower in the highly altered samples than in other, less-altered samples.

SUMMARY

Based on trace element abundances and ratios, the igneous basement in Holes 1256C and 1256D is N-MORB composition. The massive ponded flow in Hole 1256D (Unit 1256D-1) is distinct in REE abundance from flows deeper in the section, and there is a notable decrease in concentrations of all elements measured (except Pb, U, Sr, and Sc) from the base of the ponded flow in Hole 1256D to the unit immediately below the ponded flow. REE patterns for samples of basement throughout Hole 1256C are similar to those of Unit 1256D-1. The highly altered interval has significantly higher concentrations of Cs, Rb, and Ba and lower concentrations of Sr, Pb, Zr, Hf, Sc, and most REE than the samples of background alteration or halos. There are no obvious correlations of trace element abundance and macroscopic type of alteration within the samples of background alteration or halos.

ACKNOWLEDGMENTS

This research used samples and/or data provided by the Ocean Drilling Program (ODP). ODP is funded by the U.S. National Science Foundation (NSF) and participating countries under management of Joint Oceanographic Institutions (JOI), Inc. These analyses were funded by a grant from the U.S. Science Support Program. Samples were collected during ODP Leg 206. Thanks to the captain and crew of the *JOIDES Resolution* for their expertise, which made sample collection possible.

REFERENCES

Busigny, V., Laverne, C., and Bonifacie, M., 2005. Nitrogen content and isotopic composition of oceanic crust at a superfast spreading ridge: a profile in altered basalts from ODP Site 1256, Leg 206. *Geochem., Geophys., Geosyst.,* 6(12):Q12O01. **doi:10.1029/2005GC001020**

Knaack, C., Cornelius, S., and Hooper, P., 1994. Trace element analyses of rocks and minerals by ICP-MS. *Washington State Univ., Open-File Rep.*

Nakamura, N., 1974. Determination of REE, Ba, Fe, Mg, Na, and K in carbonaceous and ordinary chondrites. *Geochim. Cosmochim. Acta,* 38:757–776.

Shipboard Scientific Party, 2003. Site 1256. *In* Wilson, D.S., Teagle, D.A.H., Acton, G.D., *Proc. ODP, Init. Repts.,* 206: College Station, TX (Ocean Drilling Program), 1–396. **doi:10.2973/odp.proc.ir.206.103.2003**

Figure F1. Plots of trace element abundance vs. depth for samples analyzed. Open symbols = samples from Hole 1256C, solid diamonds = samples from Hole 1256D. Samples of the massive ponded flow (Unit 1256C-22 and Unit 1256D-1) are shown with larger symbols. Data for the chert from Hole 1256C (Sample 206-1256C-4R-1, 13–20 cm) are not plotted in order to emphasize differences between samples of the igneous basement.

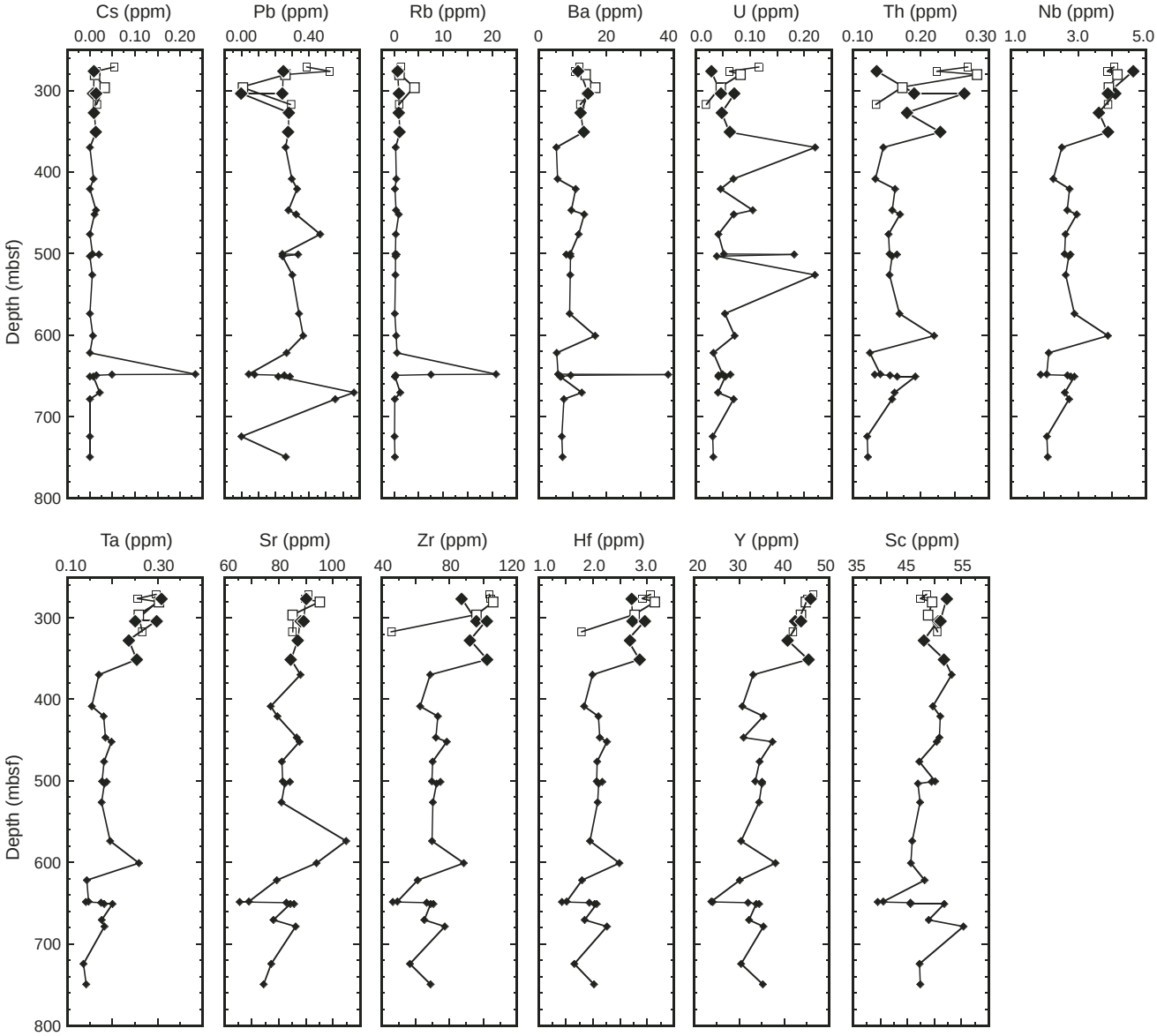

Figure F2. Plots of selected trace element ratios vs. depth. Open symbols = samples from Hole 1256C, solid diamonds = samples from Hole 1256D. Samples of the massive ponded flow (Unit 1256C-22 and Unit 1256D-1) are shown with larger symbols.

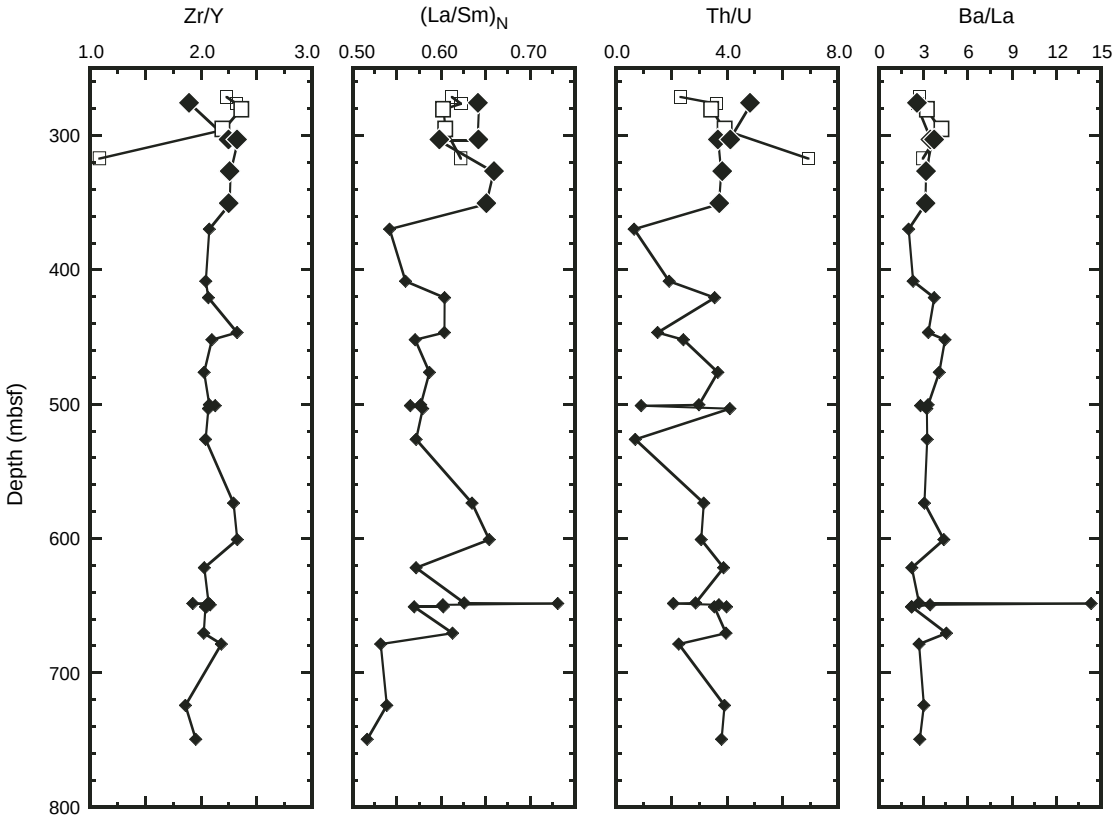

Figure F3. Diagrams showing rare earth element (REE) abundances normalized to chondritic values (Nakamura, 1974). **A.** All samples from Hole 1256C. **B.** Samples of the igneous basement in Hole 1256C (black lines and symbols), with data for the massive ponded flow in Hole 1256D shown in gray for comparison. **C–F.** Samples of igneous basement in Hole 1256D. Samples of massive ponded flow in Hole 1256D are also shown in C. Data are plotted on four diagrams in order to allow easier discrimination between samples.

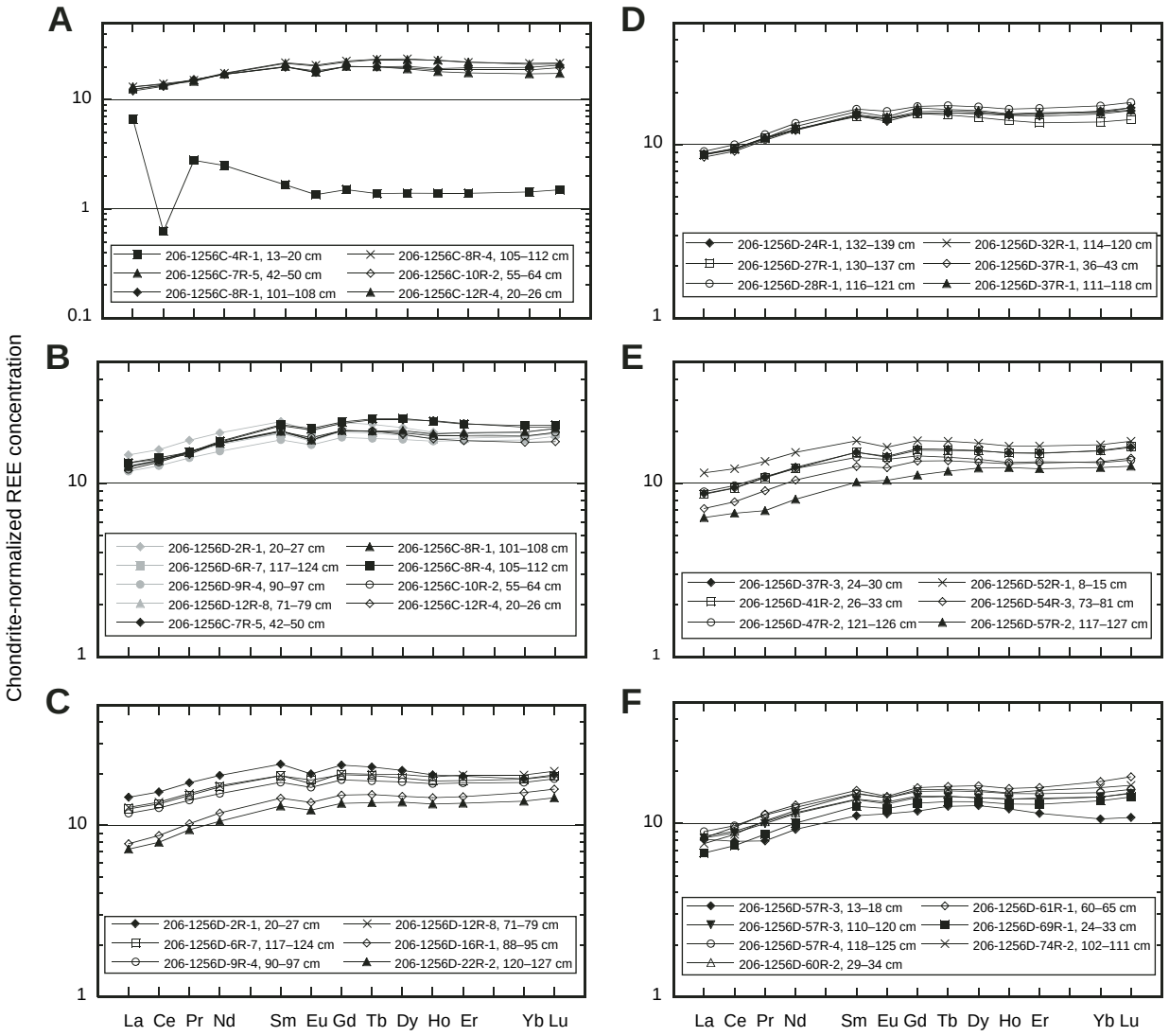

Table T1. Trace-element abundances for igneous basement at Site 1256. (Continued on next page.)

Core, section, interval (cm)	Unit*	Depth (mbsf)	Sample description	Trace elements (ppm)														
				La	Ce	Pr	Nd	Sm	Eu	Gd	Tb	Dy	Ho	Er	Tm	Yb	Lu	Ba
206-1256C-																		
4R-1, 13–20	S1	245.13	Chert	2.19	0.533	0.363	1.57	0.336	0.104	0.414	0.071	0.479	0.107	0.313	0.048	0.314	0.051	3.0
7R-5, 42–50	14	271.33	Background–cryptocrystalline basalt	4.33	11.8	1.91	10.9	4.37	1.57	6.12	1.19	7.99	1.77	4.99	0.73	4.64	0.718	12
8R-1, 101–108	15	276.51	Background–fine-grained basalt	4.09	11.6	1.99	10.7	4.05	1.37	5.57	1.02	6.92	1.49	4.41	0.66	4.35	0.703	11
8R-4, 105–112	18a	280.64	Ponded flow–cryptocrystalline basalt	4.33	12.0	1.96	11.0	4.43	1.60	6.24	1.20	8.13	1.76	4.94	0.74	4.75	0.736	14
10R-2, 55–64	18e	295.90	Ponded flow–white patchy alteration	3.96	11.3	1.96	10.7	4.04	1.41	5.57	1.02	6.71	1.45	4.23	0.63	4.13	0.667	17
12R-4, 20–26	22	317.20	Background–sheet flow below ponded flow	4.12	11.6	1.97	10.8	4.09	1.37	5.58	1.03	6.57	1.39	3.96	0.59	3.80	0.590	12
206-1256D-																		
2R-1, 20–27	1a	276.03	Ponded flow–fine-grained basalt	4.81	13.4	2.31	12.3	4.62	1.54	6.20	1.12	7.19	1.52	4.36	0.65	4.12	0.668	12
6R-7, 117–124	1c	303.71	Ponded flow–fine-grained basalt	4.10	11.4	1.95	10.6	3.95	1.42	5.45	1.00	6.49	1.40	4.11	0.62	4.09	0.658	15
6R-7, 117–124‡	1c	303.71	Ponded flow–fine-grained basalt	4.06	11.4	1.87	10.5	4.19	1.56	5.90	1.14	7.69	1.68	4.72	0.69	4.41	0.686	15
9R-4, 90–97	1c	327.27	Ponded flow–fine-grained basalt	3.86	10.8	1.82	9.66	3.62	1.28	5.08	0.928	6.15	1.35	3.98	0.59	3.92	0.634	12
12R-8, 71–79	1d	351.21	Basal unit of ponded flow–microcrystalline	4.18	11.7	2.00	10.8	3.97	1.35	5.54	1.02	6.81	1.48	4.43	0.67	4.33	0.702	13
16R-1, 88–95	3	369.78	Black halo + vein	2.57	7.46	1.33	7.43	2.92	1.05	4.14	0.773	5.07	1.12	3.30	0.50	3.41	0.552	5.2
22R-2, 120–127	4d	408.43	Mesostasis patch	2.38	6.80	1.22	6.64	2.63	0.946	3.71	0.693	4.69	1.03	3.03	0.46	3.05	0.491	5.5
24R-1, 132–139	5	420.82	Background–cryptocrystalline basalt	2.91	8.10	1.42	7.69	2.98	1.05	4.17	0.775	5.24	1.15	3.36	0.52	3.44	0.553	11
27R-1, 130–137	8a	446.70	Dark alteration near vugs	2.88	8.07	1.42	7.74	2.94	1.09	4.17	0.759	4.92	1.06	3.01	0.45	2.98	0.473	9.6
28R-1, 116–121	8a	452.06	Background–fresh cryptocrystalline basalt	3.01	8.55	1.49	8.38	3.25	1.20	4.59	0.858	5.67	1.24	3.65	0.55	3.68	0.594	13
32R-1, 114–120	8d	476.34	Background–microcrystalline basalt	2.88	7.99	1.40	7.70	3.03	1.09	4.27	0.800	5.30	1.14	3.39	0.51	3.37	0.553	12
37R-1, 36–43	10	500.46	Patchy alteration	2.79	7.83	1.38	7.62	2.98	1.08	4.16	0.779	5.16	1.14	3.29	0.50	3.30	0.532	9.3
37R-1, 111–118	10	501.21	Patchy alteration	2.88	8.15	1.42	8.02	3.14	1.11	4.50	0.815	5.40	1.16	3.44	0.51	3.38	0.535	8.1
37R-3, 24–30	10	503.29	Background–not much alteration	2.87	8.06	1.41	7.81	3.06	1.10	4.37	0.803	5.31	1.15	3.37	0.52	3.39	0.546	9.3
41R-2, 26–33	15	526.26	Background–microcrystalline basalt	2.85	8.03	1.41	7.70	3.07	1.09	4.29	0.792	5.30	1.16	3.35	0.52	3.41	0.553	9.3
47R-2, 121–126	19	573.71	Background–cryptocrystalline basalt	2.95	8.31	1.43	7.68	2.87	1.06	3.98	0.723	4.73	1.02	3.00	0.46	2.90	0.462	9.1
52R-1, 8–15	22	600.78	Background–microcrystalline basalt flow interior	3.79	10.4	1.74	9.53	3.57	1.25	4.87	0.894	5.86	1.26	3.70	0.56	3.68	0.594	17
54R-3, 73–81	23	621.76	Background–cryptocrystalline basalt	2.36	6.69	1.18	6.59	2.54	0.949	3.71	0.691	4.54	1.00	2.95	0.45	2.93	0.474	5.3
57R-2, 117–127	24a	648.02	Highly altered basalt, brick red and blue-green	2.09	5.76	0.91	5.10	2.06	0.802	3.08	0.601	4.21	0.95	2.73	0.42	2.72	0.426	5.7
57R-3, 13–18	24a	648.38	Highly altered basalt, brick red	2.67	6.75	1.03	5.84	2.25	0.877	3.26	0.643	4.35	0.93	2.58	0.37	2.34	0.368	38
57R-3, 110–120	24a	649.35	Background–coarse olivine phenocrysts	2.72	7.56	1.30	7.19	2.79	1.00	3.91	0.731	4.84	1.07	3.11	0.47	3.13	0.505	9.4
57R-4, 118–125	24b	650.83	Background, olivine-phyric	2.96	8.31	1.46	7.81	3.03	1.09	4.23	0.789	5.24	1.15	3.35	0.51	3.32	0.533	6.5
57R-4, 118–125‡	24b	650.83	Background, olivine-phyric	2.83	7.92	1.31	7.47	3.07	1.17	4.41	0.856	5.81	1.28	3.57	0.53	3.37	0.527	6.3
60R-2, 29–34	24e	670.38	Background, fine-grained	2.78	7.71	1.33	7.28	2.80	1.03	3.97	0.736	4.83	1.07	3.16	0.48	3.12	0.509	13
61R-1, 60–65	25	678.60	Halo	2.72	8.14	1.47	8.05	3.16	1.10	4.45	0.837	5.67	1.23	3.63	0.57	3.85	0.631	7.4
69R-1, 24–33	26	724.34	Background–cryptocrystalline basalt	2.23	6.38	1.13	6.34	2.55	0.941	3.62	0.684	4.59	1.00	2.91	0.45	2.98	0.482	6.8
74R-2, 102–111	26	749.56	Background–cryptocrystalline basalt	2.52	7.41	1.35	7.49	3.01	1.08	4.33	0.806	5.34	1.16	3.49	0.53	3.54	0.564	7.0
BAS-206			Leg 206 interlaboratory standard	4.89	13.86	2.37	12.82	4.79	1.62	6.60	1.18	7.88	1.67	4.81	0.736	4.68	0.758	41
Chondrite**			REE concentrations in chondrite	0.329	0.855	0.13	0.63	0.203	0.077	0.276	0.0511	0.343	0.077	0.225		0.22	0.034	

Notes: * = lithologic units defined during shipboard core description (Shipboard Scientific Party, 2003). † = La/Sm ratios normalized to chondrite. ‡ = duplicate number indicate replicate analyses using separate splits of the same powder. ** = chondrite rare earth element (REE) concentrations used in normalization (Nakamura, 1974). BD = below detection limit.

Table T1 (continued).

Core, section, interval (cm)	Unit*	Depth (mbsf)	Trace elements (ppm)																
			Th	Nb	Y	Hf	Ta	U	Pb	Rb	Cs	Sr	Sc	Zr	$(La/Sm)_N$†	Zr/Y	Th/U	Cs/Pb	Ba/La
206-1256C-																			
4R-1, 13–20	S1	245.13	0.03	0.16	4.57	0.06	0.01	0.04	2.45	0.49	0.03	28	0.54	3.2	4.01	0.70	0.80	0.01	1.4
7R-5, 42–50	14	271.33	0.27	4.06	46.5	3.06	0.30	0.12	0.39	1.37	0.05	91	48.6	104	0.612	2.23	2.3	0.14	2.8
8R-1, 101–108	15	276.51	0.22	3.87	45.1	2.91	0.26	0.06	0.52	0.71	0.01	90	47.4	104	0.622	2.32	3.6	0.03	2.6
8R-4, 105–112	18a	280.64	0.28	4.17	44.9	3.15	0.30	0.08	0.26	1.28	0.01	95	49.6	106	0.603	2.36	3.5	0.05	3.2
10R-2, 55–64	18e	295.90	0.17	3.92	43.7	2.76	0.26	0.04	BD	4.07	0.03	85	49.0	96	0.605	2.20	3.9		4.2
12R-4, 20–26	22	317.20	0.13	3.89	41.9	1.79	0.27	0.02	0.29	1.00	0.01	85	50.6	45	0.622	1.09	6.9	0.05	3.0
206-1256D-																			
2R-1, 20–27	1a	276.30	0.13	4.63	45.9	2.71	0.31	0.03	0.25	0.72	0.01	90	52.3	87	0.642	1.90	4.9	0.04	2.5
6R-7, 117–124	1c	303.71	0.19	3.88	42.5	2.74	0.25	0.05	0.24	0.97	0.01	89	51.1	96	0.641	2.26	4.1	0.03	3.5
6R-7, 117–124‡	1c	303.71	0.26	4.09	43.6	2.96	0.30	0.07	BD	1.02	0.02	88	50.6	102	0.597	2.33	3.7		3.6
9R-4, 90–97	1c	327.27	0.18	3.62	40.7	2.64	0.24	0.05	0.28	0.99	0.01	87	48.1	92	0.659	2.27	3.8	0.03	3.2
12R-8, 71–79	1d	351.21	0.23	3.88	45.4	2.86	0.25	0.06	0.28	1.18	0.01	85	51.8	102	0.650	2.26	3.7	0.05	3.2
16R-1, 88–95	3	369.78	0.14	2.52	33.1	1.99	0.17	0.22	0.26	0.33	BD	88	53.2	69	0.542	2.07	0.66		2.0
22R-2, 120–127	4d	408.43	0.13	2.27	30.7	1.84	0.15	0.07	0.30	0.46	0.01	77	49.7	63	0.560	2.04	1.9	0.03	2.3
24R-1, 132–139	5	420.82	0.16	2.75	35.4	2.10	0.18	0.05	0.33	0.18	BD	79	51.1	73	0.604	2.07	3.6		3.7
27R-1, 130–137	8a	446.70	0.16	2.68	31.0	2.13	0.18	0.11	0.28	0.41	0.01	87	50.9	72	0.603	2.32	1.5	0.05	3.3
28R-1, 116–121	8a	452.06	0.17	2.96	37.4	2.26	0.20	0.07	0.32	0.95	0.01	88	50.4	79	0.571	2.10	2.4	0.03	4.5
32R-1, 114–120	8d	476.34	0.15	2.63	34.6	2.08	0.18	0.04	0.47	0.36	BD	81	47.2	70	0.587	2.03	3.7		4.1
37R-1, 36–43	10	500.46	0.15	2.60	33.6	2.07	0.18	0.05	0.24	0.30	0.01	81	50.2	70	0.577	2.07	3.0	0.02	3.3
37R-1, 111–118	10	501.21	0.16	2.77	35.1	2.17	0.19	0.18	0.34	0.53	0.02	84	49.5	75	0.565	2.13	0.91	0.06	2.8
37R-3, 24–30	10	503.29	0.16	2.73	35.1	2.10	0.18	0.04	0.24	0.30	BD	82	47.0	72	0.579	2.07	4.1		3.2
41R-2, 26–33	15	526.26	0.15	2.64	34.4	2.09	0.18	0.22	0.30	0.27	0.01	81	47.3	70	0.572	2.04	0.70	0.02	3.3
47R-2, 121–126	19	573.71	0.17	2.89	30.5	1.94	0.19	0.05	0.34	0.15	BD	105	45.9	70	0.634	2.29	3.2		3.1
52R-1, 8–15	22	600.78	0.22	3.89	38.1	2.49	0.26	0.07	0.37	0.43	0.01	94	45.7	89	0.654	2.33	3.1	0.02	4.4
54R-3, 73–81	23	621.76	0.12	2.13	30.2	1.80	0.14	0.03	0.27	0.60	BD	79	48.2	61	0.572	2.03	3.9		2.2
57R-2, 117–127	24a	648.02	0.14	2.07	23.8	1.51	0.15	0.05	0.04	20.7	0.23	69	40.6	49	0.626	2.07	2.9	5.4	2.7
57R-3, 13–18	24a	648.38	0.13	1.90	24.2	1.42	0.14	0.06	0.08	7.5	0.05	66	39.5	47	0.731	1.93	2.1	0.63	14
57R-3, 110–120	24a	649.35	0.15	2.69	32.0	1.93	0.17	0.04	0.25	0.34	0.01	83	45.6	67	0.602	2.08	3.7	0.06	3.5
57R-4, 118–125	24b	650.83	0.17	2.79	34.4	2.03	0.18	0.04	0.29	0.18	BD	86	45.6	71	0.602	2.05	4.0		2.2
57R-4, 118–125‡	24b	650.83	0.19	2.89	33.8	2.07	0.20	0.05	0.22	0.22	0.01	84	51.8	69	0.569	2.04	3.5	0.03	2.2
60R-2, 29–34	24e	670.38	0.16	2.61	32.2	1.85	0.18	0.04	0.67	1.26	0.02	78	48.9	65	0.613	2.02	4.0	0.03	4.6
61R-1, 60–65	25	678.60	0.16	2.73	35.4	2.26	0.18	0.07	0.55	0.14	BD	86	55.4	77	0.532	2.18	2.3		2.7
69R-1, 24–33	26	724.34	0.12	2.08	30.5	1.66	0.14	0.03	BD	0.09	BD	77	47.2	57	0.539	1.86	3.9		3.0
74R-2, 102–111	26	749.56	0.12	2.11	35.3	2.02	0.14	0.03	0.26	0.17	BD	74	47.4	69	0.517	1.95	3.8		2.8
BAS-206 Chondrite**			0.26	4.56	50.2	3.34	0.58	0.25	0.47	1.82	0.05	102	55.3	121	0.631	2.40	1.1	0.12	8.4